



HOLOCENE CHRONOLOGY OF THE BRATTFORSHEDEN DELTA AND INLAND DUNE FIELD, SW SWEDEN

HELENA ALEXANDERSON¹ and DEREK FABEL²

¹*Department of Geology, Lund University, Sölvegatan 12, SE-223 62 Lund, Sweden*

²*School of Geographical and Earth Sciences, Glasgow University, Gregory Building, Glasgow G12 8QQ, United Kingdom*

Received 2 May 2014

Accepted 30 October 2014

Abstract: Brattforsheden is a large glaci-fluvial deposit in southwestern Sweden and associated with it is one of Sweden's largest inland dune fields. Although the relative ages of the Brattforsheden deposits are well known, absolute ages from the area are few. In this study we have used optically stimulated luminescence (OSL), surface exposure (¹⁰Be) and radiocarbon (¹⁴C) dating to provide an absolute chronology for the deglaciation and for the Holocene development of the aeolian dunes. Our data show that the deglaciation took place just before 11 ka (11.5 ± 0.6 ka OSL, 11.3 ± 0.8 ka ¹⁰Be), in line with the ¹⁴C-based regional deglaciation age. Aeolian dunes started forming immediately after deglaciation and were active for at least 2000 years, well after vegetation had established. Renewed aeolian activity occurred 270–180 years ago, resulting in the deposition of sand sheets. Comparison between dating methods and studies of OSL dose distributions show that glacial, glaci-fluvial and littoral sediments suffer from incomplete bleaching and thus that mean OSL ages from such deposits overestimate the true depositional age. By using small aliquots and statistical age models, this effect can partly be countered. Also, some of the ¹⁰Be ages appear too old, which may be due to previous exposure.

Keywords: luminescence (OSL) dating, surface exposure dating (¹⁰Be), deglaciation, aeolian, Holocene, Sweden.

1. INTRODUCTION

The successive retreat of the ice margin during the deglaciation in south western Sweden is spatially well constrained by moraines and ice-marginal glaci-fluvial deposits (Lundqvist and Wohlfarth, 2001). However, north of the Middle Swedish End Moraine Zone, at and above the highest shoreline, the deglacial geomorphological record is much more discontinuous and the deglaciation chronology is less well known (Lundqvist, 2002). One of the major deglacial features in this area is the Brattforsheden delta, which formed at the Yoldia Sea

coast as the ice margin crossed the highest shoreline and adapted itself from marine to terrestrial mode of deglaciation (Fredén, 2001a). The range of deglacial and paraglacial deposits at Brattforsheden (tills, deltas, beaches, dunes) makes it a good target for dating the deglaciation, and an interesting case study for comparing deglaciation ages from different types of deposits and from different techniques.

Three common methods for dating the deglaciation are radiocarbon (¹⁴C), optically stimulated luminescence (OSL) and surface exposure (¹⁰Be) dating. However, these methods do not necessarily date the same event. ¹⁴C dating generally provides ages of the first organic sedimentation after the ice sheet disappeared, and thus gives minimum ages for the deglaciation — the lag between melting of ice and establishment of vegetation is not necessarily known. OSL, on the other hand, dates the last

Corresponding author: H. Alexanderson
e-mail: helena.alexanderson@geol.lu.se

time sediment was exposed to sunlight, which is assumed to be the time of deposition. For glaciofluvial deposits this would be at the time of ice-margin retreat and OSL would therefore provide accurate ages of deglaciation. There may, however, be problems with age overestimation due to incomplete bleaching in some depositional environments (Singarayer *et al.*, 2005; Alexanderson and Murray, 2012a). Surface exposure dating gives the duration of exposure at the surface of, for example, glacially deposited boulders, which would translate to an accurate age of ice disappearance, if the boulder was not previously exposed, subsequently exhumed or covered by, for example, sediment or snow. The resolution of the three methods also typically differ, with ^{14}C being more precise (typically $\sim 2\%$ for deglaciation ages) and OSL and ^{10}Be less precise ($\sim 5\text{--}10\%$). However, if the ages fall on a ^{14}C plateau, the precision of calibrated ^{14}C ages is reduced. In this study, we will mainly evaluate ^{10}Be and OSL ages of the deglaciation and related events.

One of the best developed aeolian dune fields in Sweden is located at Brattforsheden (Bergqvist, 1981), but not much is known about its development during the Holocene. The chronology of aeolian deposits in Sweden is largely non-existent; most have been assumed to have formed immediately after deglaciation (Högbom, 1923; Hörner, 1927; Seppälä, 1972; Bergqvist, 1981), but very few absolute ages are available. At some sites there is evidence of more recent aeolian activity (Högbom, 1923; Bergqvist, 1981), but the timing of those events is also poorly constrained. In many aspects, the Brattforsheden dune field is similar to many other inland dune fields in Scandinavia (Klemsdal, 1969; Seppälä, 1972; Bergqvist, 1981), particularly in southern Sweden and Norway, and better knowledge of its development has implications for similar landforms elsewhere.

The main aim of this paper is to better constrain the absolute chronology of the Brattforsheden delta and inland dune field, thereby providing improved age control of the deglaciation in the area and presenting the first more extensive chronology of an inland dune field in Sweden. A second aim is to explore the absolute age relationship between different types of deglaciation deposits. This is achieved by OSL dating of glacial, glaciofluvial, wave-washed and aeolian sand, by ^{10}Be dating of glacially deposited boulders and by ^{14}C dating of organic material from a palaeosol. Many of the OSL ages presented here have previously been used to evaluate bleaching in different depositional environments and the luminescence characteristics of Swedish quartz (Alexanderson and Murray, 2012a), but their sedimentological context and geological implications have previously not been described and discussed.

2. STUDY AREA AND PREVIOUS INVESTIGATIONS

The Brattforsheden delta and its dune field have been beautifully mapped by Hörner (1927) and the area is also at least partly covered by three generations of Quaternary deposits maps from the Geological Survey of Sweden in scales from 1:200000 to 1:50000 (Magnusson and Assarsson, 1929; Lundqvist, 1958; Fredén, 2001b).

The delta is part of a large glaciofluvial deposit, formed at the highest shoreline 175–190 m a.s.l. during the last deglaciation of SW Sweden (Fig. 1). The deposit follows a NNW-SSE directed, structurally controlled valley and includes deltas, terraces, kames, kettle holes and eskers. The main delta surfaces, approximately 15 km² in area, are found at the valley mouth in the south, where sediment thicknesses of more than 100 m have been documented (Aneblom and Åsman, 2000). A feeding esker follows the central part of the valley, today occupied by Lake Alstern (Fig. 1). The surrounding hills are covered by a relatively thin till layer, which in a few places form small moraine ridges and hummocks.

As land rose out of the sea due to isostatic rebound, the deltaic sediments and the surrounding till were wave-washed, and gullies developed at and in front of the delta slope. Aeolian dunes also formed on the delta surface and at the northern end of Lake Alstern (Hörner, 1927; Fredén, 2001a), as can be seen in Fig. 1. The aeolian deposits at Brattforsheden form dunes, cover sands and loess-like covers. The dunes are mainly crescentic to parabolic and most of the large dunes are found just NW and SE of Lake Alstern, respectively (Fig. 1). Smaller dunes and cover sand are found in many places, in close association with glaciofluvial sediments. The loess-like deposits (*flygmo* in Swedish) consist of fine sand and coarse silt and form thin covers on surrounding elevations, up to ~ 290 m a.s.l. (Hörner, 1927; Fredén, 2001a).

The deglaciation chronology of the area, and thus the formation time of the delta, is relatively poorly constrained. Correlation with clay-varve- or ^{14}C -dated recession lines in eastern Sweden and in southern Norway, together with ^{14}C -ages of early organic sedimentation in lake basins in the region, suggest that deglaciation took place ~ 10.9 cal ka BP (no uncertainty stated; Fredén, 2001a; Lundqvist, 2002). It has generally been assumed that the aeolian deposition took place immediately after deglaciation (Hörner, 1927). This is supported by two thermoluminescence (TL) ages that show aeolian deposition occurred around ~ 9000 years ago (Table 1; Lundqvist and Mejdahl, 1987). Reactivation of at least some dunes took place in historical times (< 500 cal yr BP), as shown by ^{14}C -ages from a palaeosol in one of the dunes and a TL age from the overlying sand (0.85 ± 0.3 ka, Table 1; Bergqvist and Lindström, 1971; Lundqvist and Mejdahl, 1987).

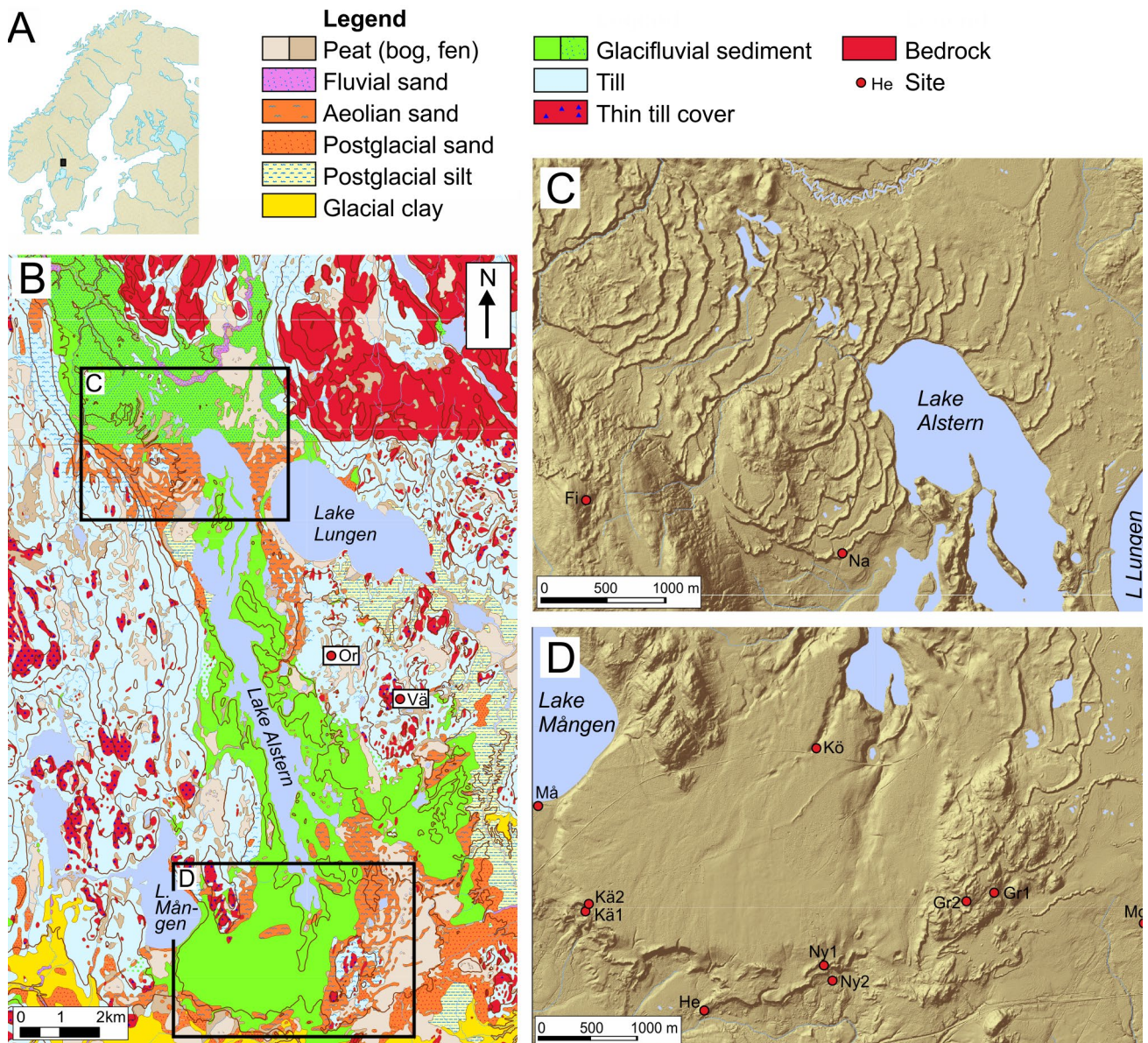


Fig. 1. A. Overview map showing the location of Brattforsheden in western Sweden (black square). B. Geological map of the Brattforsheden delta and surroundings. Note that the sharp horizontal boundary in the upper quarter of the map is artificial, due to base maps of different scale and symbology. Geological data are copyright of the Geological Survey of Sweden, permission no. 318-2255/2013. C. Hillshade digital elevation model of the northern part of the area with the main dune field. D. Hillshade model of the southern part of the area, with the main delta surface. Elevation data in C and D are copyright of Lantmäteriet, permission no. i2012/927. On the maps, sites are identified by the first two letters in their name.

Table 1. Previously published ages from sites investigated in this study. Note that Långbromana (Bergqvist and Lindström, 1971), Västerrud (Lundqvist and Mejdahl, 1987) and Nabbmanen (this study) are the same site. A. Radiocarbon ages, calibrated by us in OxCal 4.2 online and using the IntCal13 calibration curve (Bronk Ramsey, 2009; Reimer et al., 2013). Lab numbers not given in the original publication. B. Thermoluminescence ages.

A. Radiocarbon ages from Långbromana

Sample no.	Lab. no.	Material	¹⁴ C age (BP)	Calibrated age (BP)	Reference
Prov A	Ua-n/a	coal-like material	2940 ± 90	3345–2870	Bergqvist and Lindström (1971)
Prov B	Ua-n/a	charcoal	500 ± 70	659–331	Bergqvist and Lindström (1971)

B. Thermoluminescence ages on 0.1-0.3 mm K feldspar grains from aeolian material

Sample no.	Lab. no.	TL age (ka)	Dose (Gy)	Dose rate (Gy/ka)	Reference
Finnhöjden	R841609	9.0 ± 0.7	39	4.35	Lundqvist and Mejdahl (1987)
Västerrud 1	R841610	0.85 ± 0.3	4.2	4.95	Lundqvist and Mejdahl (1987)
Västerrud 2	R841611	9.1 ± 0.7	44.4	4.89	Lundqvist and Mejdahl (1987)

3. METHODS

Field work

Field work was carried out in summer 2006. Sites for sampling were selected based on geological and geomorphological maps (Hörner, 1927; Fredén, 2001a, 2001b) and a survey of the area. The sites included gravel pits, road cuts and hand-dug pits (Table 2). Each site was documented by sedimentological logging, and positions and elevations were determined by a handheld Garmin GPS Vista C (precision ± 5 m).

Samples for luminescence dating were taken by hammering opaque plastic tubes into the sediments. The tubes were stored in black plastic bags until opened under darkroom conditions. Pieces of charcoal for radiocarbon

dating were picked from excavated sections and stored in plastic bags. Rock samples for surface dating were chipped from the top part of boulders by using hammer and chisel. Shielding from the surrounding horizon was measured with a compass and clinometer.

Luminescence dating

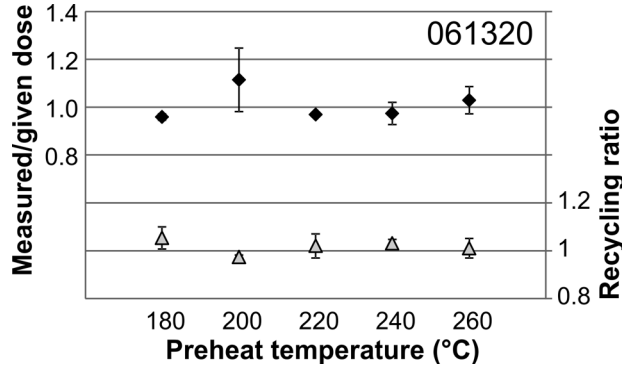
The luminescence samples were prepared and measured at the Nordic Laboratory for Luminescence Dating (NLL) at Risø, Denmark in 2006–2007. Complementary measurements on samples 061311, -14, -15, -17, -19 and -21 were carried out at the Lund Luminescence Laboratory in 2012 and 2013. Preparation included standard treatment with 10% HCl to remove carbonates, 10% H₂O₂ to remove any organic material and 38% HF to

Table 2. Sites investigated in this study, see also Fig. 1.

Site	Latitude (deg. N)	Longitude (deg. E)	Elevation (m a.s.l.)	Type	Samples
Finnhöjden	59.72165	13.84056	270	road cut	OSL 061311
Gräshöjden 1	59.60853	13.95843	202	hand-dug pit	OSL 061312
Gräshöjden 2	59.60770	13.95336	211–212	road cut	OSL 061313-14
Hedbacka	59.59732	13.90591	145	hand-dug pit	OSL 061315
Källorna 1	59.60648	13.88337	167–175	gravel pit	OSL 061316-19,-22
Källorna 2	59.60720	13.88415	175	hand-dug pit	OSL 061320-21
Köldgropen	59.62154	13.92524	182	hand-dug pit	OSL 061323
Mosserud	59.60569	13.98647	173	hand-dug pit	OSL 061324
Mången	59.61602	13.87416	167	wave-eroded cut	OSL 061325
Nabbmanen	59.71782	13.87360	172–173	road cut	OSL 061326-30
Nyången 1	59.60168	13.92771	173–174	road cut	OSL 061331-32
Nyången 2	59.60042	13.92906	158	hand-dug pit	OSL 061333
Ormtjärnen 1	59.68048	13.94212	185	boulder on end moraine	¹⁰ Be ORM-1A,B
Ormtjärnen 2	59.68048	13.94187	184	boulder on end moraine	¹⁰ Be ORM-2A,B
Ormtjärnen 3	59.68053	13.94210	185	boulder on end moraine	¹⁰ Be ORM3
Västra höjden 1	59.67028	13.96887	225	road cut	OSL 061334
Västra höjden 2	59.66998	13.96845	225	boulder on moraine hummock	¹⁰ Be VÅS-2
Västra höjden 3	59.67063	13.96810	225	boulder on moraine hummock	¹⁰ Be VÅS-3
Västra höjden 4	59.67090	13.96892	224	boulder on moraine hummock	¹⁰ Be VÅS-4

Table 3. SAR protocol settings used for OSL analyses.

Group	Sample	Preheat (°C)	Cutheat (°C)	Test dose (Gy)
A	061311-14,20-21,23,31-32	260	220	5–10
B	061326-27	220	180	5–6
C	061322,25,28,29,30	180	160	1–2

**Fig. 2.** The dose recovery analysis at different preheat temperatures of sample 061320 shows that the dose recovery ratio is largely independent of temperature. This plot is representative for samples in group A (Table 3).

remove remaining impurities and also to etch the outer surface of the grains. A magnet was used to remove any magnetic grains. IR-tests (Duller, 2003) showed that the infrared/blue ratio was on average $3.1 \pm 0.3\%$, indicating insignificant feldspar contamination. Water content was measured on subsamples taken from the ends of the sample tubes. The selection of the average water content for age calculation was based on the depth and location of the sample relative to the expected groundwater level. The environmental dose rate was determined by gamma spectrometry (Murray *et al.*, 1987) and by calculating the contribution from cosmic radiation according to Prescott and Hutton (1994).

OSL measurements were done on large (8 mm) and small (2 mm) aliquots of 180–250 μm quartz grains with Risø TL/OSL readers equipped with $^{90}\text{Sr}/^{90}\text{Y}$ beta radia-

tion sources (dose rate 0.10–0.33 Gy/s), blue ($470 \pm 30 \text{ nm}$; $\sim 50 \text{ mW/cm}^2$) light sources, and detection was through a 7 mm U340 glass filter. All samples were analysed with SAR-protocols (Murray and Wintle, 2000, 2003) adapted for each sample on the basis of dose recovery analysis (Table 3, Fig. 2).

The OSL signal was integrated from channels 1 to 5 (the first 0.8 s) for most samples and the background was taken from channels 6 to 10 (the next 0.8 s); for samples 061311–13 channels 1–10 (first 1.6 s) and 26–50 were used instead as it gave better dose recovery. Aliquots were accepted if recycling ratio was within 10% of unity, test dose error $<10\%$ and the signal more than three standard deviations above the background. The dose was calculated using exponential curve fitting in Risø Analyst v. 3.24. For the small-aliquot data, the single-aliquot decision protocol of Arnold *et al.* (2007) was followed and the three-parameter minimum-age model (MAM-3; Galbraith *et al.*, 1999) was applied to the data by using an excel macro constructed by Sebastien Huot, after adding a 10% uncertainty (determined from the overdispersion of dose-recovery results) to each value.

The mean dose recovery ratio for the large aliquots is 1.04 ± 0.01 ($n = 47$) and for the small aliquots 1.06 ± 0.03 ($n = 9$). Mean recycling ratio for all accepted aliquots is 1.005 ± 0.003 ($n = 757$) and recuperation was low ($<5\%$ of natural). Thermal transfer tests made for a few aliquots of samples measured with 260°C preheat show a mean transferred dose of 0.7 Gy ($n = 3$), which is much less than the D_c 's ($>30 \text{ Gy}$) and is considered insignificant.

Surface exposure dating

Rock samples for ^{10}Be dating were crushed at the Natural History Museum in Stockholm and sieved at Stockholm University. Further preparation and analysis was performed at the Glasgow University Cosmogenic Nuclide Laboratory in Scotland. Preparation included processing for ^{10}Be from quartz following procedures modified from Kohl and Nishiizumi (1992) and Child *et al.* (2000). The samples were measured at the Scottish Universities Environmental Research Centre AMS La-

Table 4. Surface exposure sample analytical data and ^{10}Be concentrations.

Sample ID	Quartz mass ^a (g)	^9Be carrier (μg)	$^{10}\text{Be}/^9\text{Be}^{\text{a,b}}$ ($\times 10^{-15}$)	Blank $^{10}\text{Be}/^9\text{Be}^{\text{a,b}}$ ($\times 10^{-15}$)	$[^{10}\text{Be}]^{\text{c}}$ ($10^4 \text{ atom g}^{-1} \text{ SiO}_2$)
ORM-1A	26.381	253.4 ± 5.1	85.32 ± 3.60	2.66 ± 0.72	5.82 ± 0.30
ORM-1B	19.980	253.1 ± 5.1	66.29 ± 3.39	2.66 ± 0.72	5.91 ± 0.36
ORM-2A	23.233	254.0 ± 5.1	82.18 ± 3.95	2.66 ± 0.72	6.37 ± 0.36
ORM-2B	12.559	253.8 ± 5.1	44.40 ± 2.63	4.75 ± 0.85	5.87 ± 0.46
ORM-3	25.859	252.1 ± 5.0	111.9 ± 19.4	2.66 ± 0.72	7.81 ± 1.40
VÄS-2	15.836	256.7 ± 5.1	65.18 ± 2.93	2.66 ± 0.72	7.43 ± 0.41
VÄS-3	26.474	253.4 ± 5.1	99.67 ± 4.74	3.45 ± 0.72	6.75 ± 0.37
VÄS-4	17.692	254.6 ± 5.1	66.29 ± 2.41	2.66 ± 0.72	6.71 ± 0.32

^a Isotope ratios normalized to NIST SRM4325 with a value of 2.79×10^{-11} (Nishiizumi *et al.*, 2007).

^b Uncertainties are reported at the 1s level and include all known sources of analytical uncertainty (blank, carrier mass and counting statistics).

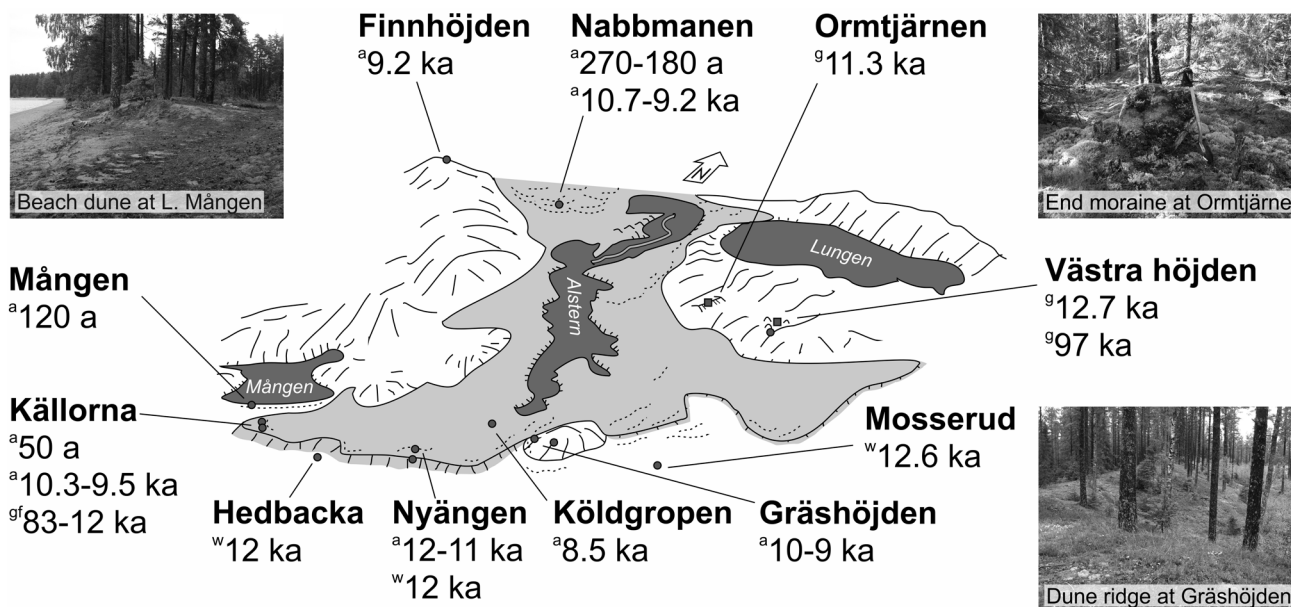


Fig. 3. Schematic birds-eye view of the Brattforsheden area showing relative location of sites and a summary of ages. The grey colour represents the glacialfluvial deposits and the hatched lines are dunes. Superscript letters show type of deposited dated: a — aeolian, w — wave-washed, gf — glacialfluvial, g — glacial. All ages are OSL ages except the one from Ormtjärnen and the young one from Västra höjden, both of which are ¹⁰Be ages.

boratory. Measured ¹⁰Be/⁹Be ratios were corrected by full chemistry procedural blanks (Table 4). We calculated the analytical uncertainty by assuming that the uncertainties in AMS measurement and Be carrier are normal and independent, adding them in quadrature in the usual fashion (e.g. Bevington and Robinson (1992)). The resulting analytical uncertainties range from 5 to 7% (Table 4), except for ORM-3.

Measured ¹⁰Be concentrations were used to calculate surface exposure ages using the CRONUS-Earth ¹⁰Be–²⁶Al exposure age calculator version 2.2 (<http://hess.ess.washington.edu>), assuming no prior exposure and no erosion during exposure. The calculator provides a variety of production rate calibrations, and we used the Arctic calibration (Young *et al.*, 2013) with a spallation-induced production rate of 3.93 ± 0.15 atoms $g^{-1} a^{-1}$ (CRONUS-Earth 2013; Alternate calibration data sets, Wrapper script 2.2, Main calculator 2.1, constants 2.2.1, muons 1.1). This production rate was chosen because the calibration data set extends back to ca. 16 ka, compared to 12 ka for the northern Norway and western Norway production rate calibrations of Fenton *et al.* (2011) and Goehring *et al.* (2012a, 2012b).

Radiocarbon dating

One sample of charcoal was submitted to the Radiocarbon Laboratory at Lund University for radiocarbon dating. Two unpublished ages of terrestrial macrofossils from a core from a nearby lake (Lake Falltjärnen), 15 km ENE of the northern end of Lake Alstern, were also made available, courtesy of Jan Risberg, Stockholm University.

4. RESULTS

Sites and sediments

In total 13 sites were investigated: most were in the southern part of the Brattforsheden area, at or on the delta plateaux, two were at the northern end of Lake Alstern and two on the till-covered hills east of Lake Alstern (Fig. 1, Fig. 3, Table 2).

Glacial deposits

The OSL sample was taken from a massive matrix-supported sandy diamicton, situated above the highest shoreline at Västra höjden (Fig. 3) and it has therefore not been affected by wave action. It is interpreted as a till, but from the limited exposure available it is difficult to determine its genesis; much of the till in the area is subglacially deposited, but nearby, at slightly higher elevation, a patch of hummocky moraine indicates a dead-ice landscape with possible melt-out or flow till.

Three boulders were sampled for ¹⁰Be dating from the forested hummocky moraine at Västra höjden. The boulders are 125–180 cm high and consist of gneiss (VÄS2, VÄS4) or granite (VÄS3) (Fig. 4A–C). A few kilometres to the northwest is Ormtjärnen (Fig. 3), where there is a small end moraine. Three 65–110 cm high granitic boulders on the crest of the moraine were sampled (Fig. 4D–E). All boulders appeared to be only slightly weathered or eroded, although they are partly covered by moss or lichen. However, boulder ORM1 has a 2-mm weathering rind. At both sites, the erratics are situated on low-relief, well-drained sandy till.

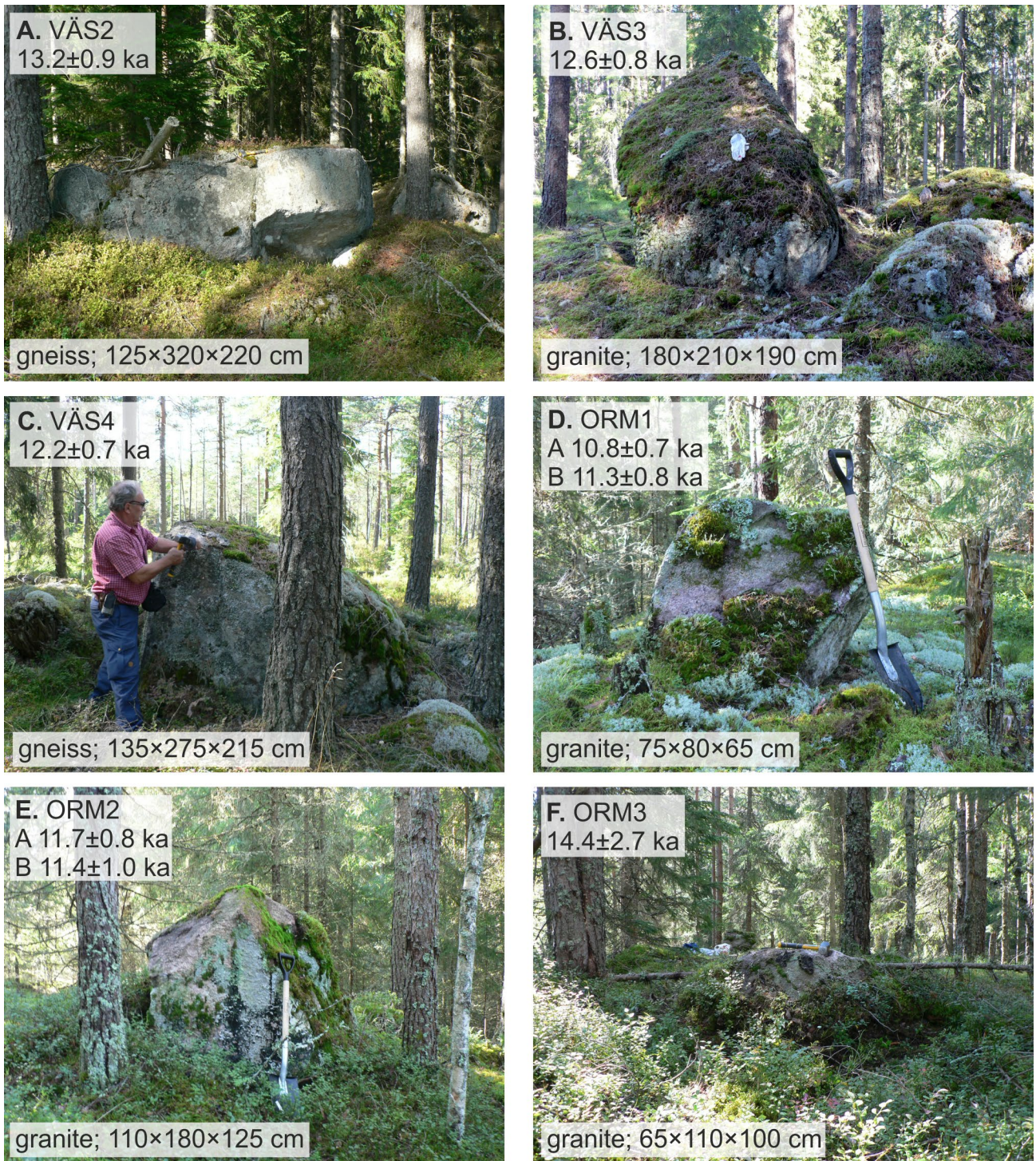


Fig. 4. The boulders that have been ^{10}Be dated. A-C. VÄS1-3 from hummocky moraine at Västra höjden. D-F. ORM1-3 from an end moraine at Ormtjärnen. Size given as height × length × width.

Deltaic deposits

The deltaic deposits were documented at the Källorna gravel pit (Fig. 1), where they are partly exposed in 10–15 m high scree-covered sections (Fig. 5). The sandy beds in the section dip S-SW; the dip decreases upwards (Fig. 5A). The most common sedimentary structures are

planar lamination, ripple lamination and massive. The sediments are interpreted as delta slope deposits (lower part) and as channels on the delta topset (upper part). The topmost sediments have been disturbed and possibly moved around during excavation.

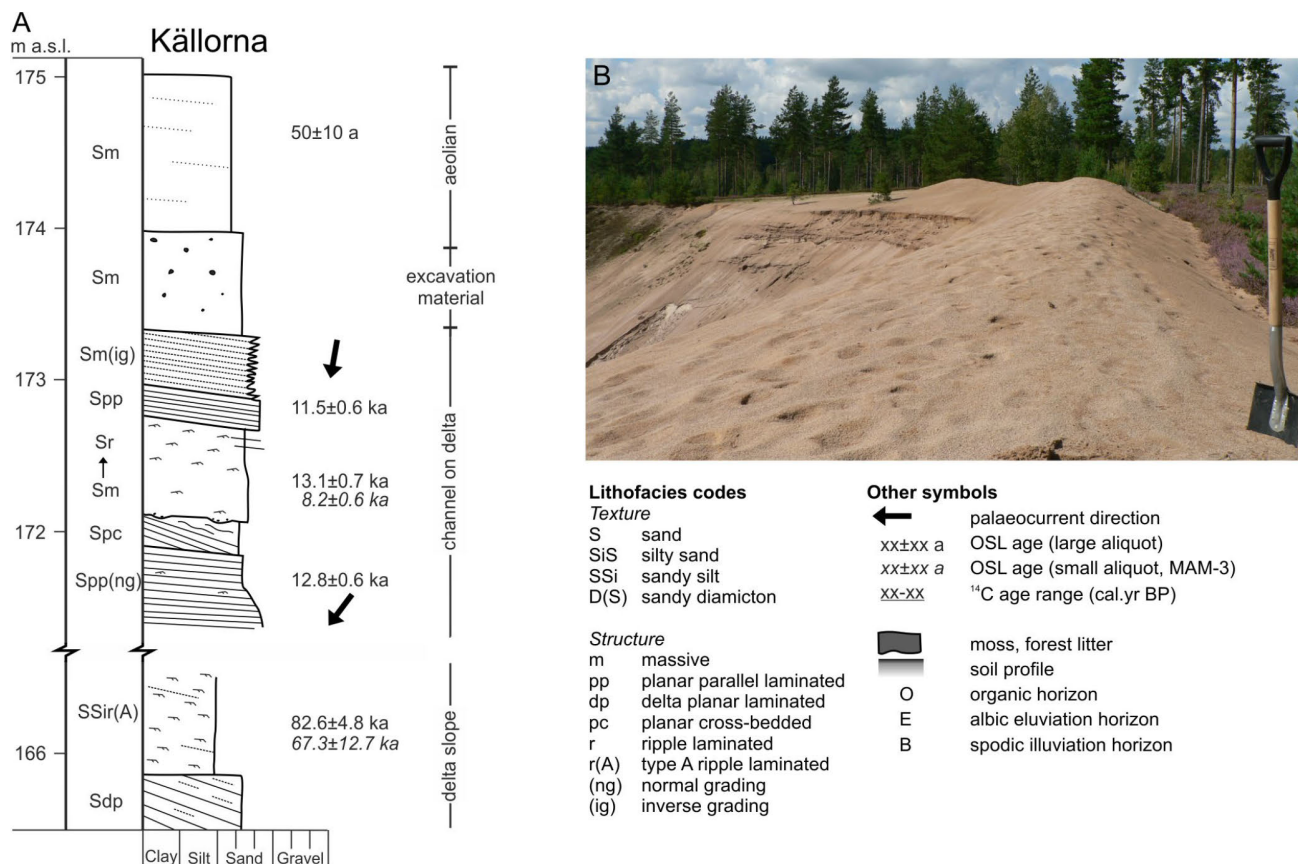


Fig. 5. A. Composite log from the Källorna site. B. The small cliff-top dune forming at the edge of the active gravel pit, and which was sampled as a modern analogue. The deltaic sediments below are visible to the left. The legend applies also to Fig. 6 and Table 5.

Wave-washed sediments.

The three sites Hedbacka, Nyängen 2 and Mosserud are situated below the highest shoreline and are, according to the geological map (Fredén, 2001b), covered by postglacial sand. The fine- to medium-grained sand appeared massive in the hand-dug pits, but some stratification is suggested by occasional finer-grained lamina. Exposures may have been too small to securely discern any large-scale stratification. Nevertheless, the well-sorted sand in combination with the geomorphology, including a beach terrace at Hedbacka, supports a littoral origin of these sediments.

Aeolian sediments

The best exposure is at Nabbmanen, at the northern end of Lake Alstern, where a road cuts through a long sinuous dune (Fig. 1). In the lower part of the road-cut section the fine-medium sand is cross-stratified and well-sorted, and dips ~20° towards the SW. Massive sand dominates the upper part (Fig. 6). The cross-stratified sand is interpreted as dune foresets, formed on the lee side of the dune, while the massive sand represents a sand sheet covering the dune. The cross-stratified and the massive sand are separated by an interval with white- and

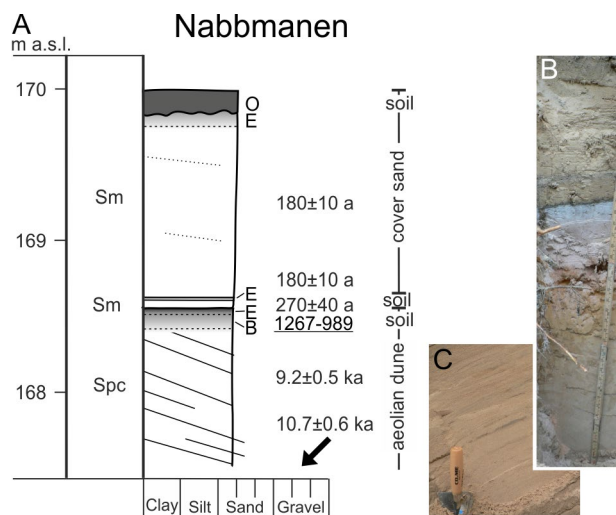


Fig. 6. A. Log from the Nabbmanen site. For legend see Fig. 5. B. The central part of the logged section, including the soils at 168.5 m a.s.l. C. The cross-bedded dune sand in the lower part of the logged section.

red-coloured sand, interpreted as at least one palaeosol (Fig. 6). The lower paleosol has a ~8 cm thick eluviation (E) horizon, and an at least 20 cm thick B horizon, which

gradually fades downwards. Five cm above this paleosol is a 1 cm thick whitish lamina, which may be a remnant of a second palaeosol. At Nabbmanen, there is thus evidence of dune formation, landscape stabilisation with soil formation and then renewed aeolian activity with deposition of a sand sheet.

Dunes at Gräshöjden 2, Nyängen 1 and Källorna 2 were also investigated. The three sites represent different dune types or settings: the Gräshöjden 2 dune is a pronounced ridge located in higher terrain, the Nyängen 1 dune is also geomorphologically well-defined but situated at the distal margin of the delta, and the Källorna 2 dune is situated on the delta plain but is not very prominent. Exposures were poor, but all sites showed well-sorted, vaguely laminated fine-medium sand that in connection with the geomorphological context was interpreted as dune sand.

At the Källorna gravel pit, there is a low ridge, which follows the edge of the gravel pit (**Fig. 5B**) and which is formed on top of excavation material. Its surface is rippled and it is interpreted as a recently formed, still active small cliff-top dune. Yet another type of dune was studied at Lake Mången, where a low (<1 m) winding ridge parallels the present beach for >500 m. The ridge contained massive sand, and is interpreted as a beach dune. It was described as partly active in the early 20th century by Hörner (1927).

Köldgropen is a flat area at the head of a large gully leading into Lake Alstern (**Fig. 1**). A hand-dug pit revealed almost a metre of well-sorted, vaguely laminated fine-medium sand, very similar to the sand seen at Nabbmanen, and interpreted as cover sand. There was a forest fire here in 1911 (Sven-Åke Berglind, pers.comm. 2006), but no signs of charcoal was found in the sediment.

At two sites, Finnhöjden and Gräshöjden 1, massive coarse silt/fine sand on top of till is interpreted as loess-like deposits.

Luminescence ages

The mean large-aliquot OSL ages for samples measured at the two different laboratories (NLL and Lund) overlap within error (**Table 5**) and indicate good reproducibility of the measurements. Three of the four small-aliquot mean ages are on average 10% lower than the large-aliquot mean ages, but their age distributions overlap; the fourth agrees very well with the large-aliquot data. The environmental dose rates average 3.8 Gy/ka (3.22–4.49 Gy/ka) and OSL equivalent doses span from ~440 Gy to 0.2 Gy (**Table 5**). The resulting ages range

from 97 ka to 50 a (**Table 5, Fig. 3, Fig. 5, Fig. 6**). The dose distributions for the four small aliquot measurements are relatively wide (overdispersion 21–42%; cf. $7 \pm 2\%$ for dose recovery) and also skewed (**Fig. 7**).

The quartz was generally fairly bright and had a clear fast signal component, but about 10% of the aliquots were rejected mainly due to poor recycling ratios. For further information on the luminescence characteristics of these samples the reader is referred to Alexanderson and Murray (2012a).

The OSL ages are stratigraphically consistent and where independent age control is available, the OSL ages agree with that data (Lake Mången and Nabbmanen sites). From a chronological point of view, the ages cited in the text below are generally the large-aliquot ages determined at the NLL. These are measured on more aliquots than the corresponding measurements in Lund and are thus expected to have a slightly higher precision and accuracy. For the small aliquots, it is the modelled (MAM-3) ages that are referred to when discussing timing.

Surface exposure ages

The seven ¹⁰Be ages range from 10.8 to 14.4 ka (**Table 6**). For the two cases where two samples were taken from the same boulder (ORM-1A and -1B, ORM-2A and -2B) the two ages overlap within analytical uncertainty. Sample ORM-3 produced a Be current an order of magnitude lower than average (3–4 μ A) during AMS measurement resulting in larger AMS counting uncertainty ($\pm 17\%$) compared to the other samples ($\pm 5\%$ on average) and ORM-3 is therefore excluded from further interpretation.

The ages from the Ormtjärnen site are on average slightly younger (11.3 ± 0.8 ka; excluding ORM-3) than the ages from Västra höjden (12.7 ± 0.8 ka). These ages were conservatively calculated assuming no erosion and no correction for cover by snow or trees. If instead 1.0 mm/kyr erosion and cover by trees (0.977 correction factor; Plug *et al.* (2007)) and snow (40 cm with density 0.25 g cm^{-3} for 4 months per year; SMHI (2014)) were assumed, the average ages become 11.8 ± 0.6 ka and 13.2 ± 0.9 ka, respectively.

Radiocarbon ages

The lowest and thickest paleosol at Nabbmanen is dated to 1270–990 cal years BP (NAB-6; **Table 7, Fig. 6**). The macrofossils from Lake Falltjärnen date the isolation of the lake from the Yoldia Sea to 10.6–10.3 cal ka BP (**Table 7**; Jan Risberg, pers.comm. 2008). Lake Falltjärnen has a threshold level at 160–165 m a.s.l.

Table 5. OSL data for samples measured at the Nordic Laboratory for Luminescence dating and at the Lund Luminescence Laboratory.

Sample no.	Site	Deposit	Lithofacies ^a	Depth (cm)	Type ^b	Age (ka)	Dose (Gy)	Dose rate (Gy/ka)	acc. n/total n ^c	OD ^d	w.c. (%)
061311	Finnhöjden	aeolian	SSim	55	LA-R	9.2±0.6	29.7±1.3	3.24±0.12	20/23	18±3	24
					LA-L ^e	9.2±0.6	30.2±1.4	3.27±0.12	11/12	16±4	24
061312	Gräshöjden 1	aeolian	SiSm	45	LA-R	9.6±0.5	35.8±0.9	3.74±0.15	21/27	8±2	17
061313	Gräshöjden 2	aeolian	Sm	110	LA-R	10.0±0.5	34.5±0.6	3.45±0.14	23/30	4±2	11
061314	Gräshöjden 2	aeolian	Sm	65	LA-R	9.0±0.5	33.4±0.7	3.69±0.15	21/24	8±2	9
					LA-L	10.2±0.7	37.7±1.7	3.69±0.15	11/12	13±3	9
061315	Hedbacka	wave-washed	Sm	50	LA-R	12.0±0.6	41.5±1.2	3.47±0.14	21/27	9±2	15
					LA-L ^e	12.5±1.7	43.8±5.4	3.50±0.14	11/12	33±7	15
					SA-L	10.9±0.6	37.9±0.9	3.47±0.14	87/96	21±2	15
					SA-M	9.5±1.2	33.0±4.0	3.47±0.14	p=0.5		15
061316	Källorna 1	delta	Spp	100	LA-R	11.5±0.6	50.3±0.8	4.37±0.18	24/24	5±2	12
061317	Källorna 1	delta	Sr	200	LA-R	13.1±0.7	51.3±1.3	3.93±0.17	24/24	10±2	11
					LA-L ^e	13.1±0.9	52.2±2.4	3.97±0.17	12/12	13±3	11
					LA-L ^e	13.5±0.8	53.7±1.4	3.97±0.17	65/66	28±3	11
					SA-M ^e	8.2±0.6	32.7±1.8	3.97±0.17	p=0.018		11
061318	Källorna 1	delta	Spp	300	LA-R	12.8±0.6	45.5±0.8	3.55±0.14	24/24	7±2	14
061319	Källorna 1	delta	SSir	800	LA-R	82.6±4.8	281.5±10.5	3.41±0.14	24/24	11±2	20
					SA-L	74.4±6.0	253.6±17.1	3.41±0.14	42/45	42±5	20
					SA-M	67.3±12.7	229.4±42.0	3.41±0.14	p=1.0		20
061320	Källorna 2	aeolian	Sm	60	LA-R	10.3±0.6	38.2±1.3	3.72±0.16	21/24	14±3	8
061321	Källorna 2	aeolian	Sm	50	LA-R	9.5±0.6	39.7±1.9	4.17±0.18	17/18	28±3	9
					LA-L	8.8±0.8	36.5±2.7	4.17±0.18	12/12	25±5	9
					SA-L	8.2±0.4	34.1±0.9	4.17±0.18	82/126	27±2	9
					SA-M	7.8±1.0	32.6±3.8	4.17±0.18	p=0.9		9
061322	Källorna 1	aeolian	Sm	40	LA-R	0.05±0.01	0.21±0.03	4.17±0.17	13/24	0	11
061323	Köldgropen	aeolian	Sm	55	LA-R	8.5±0.5	35.0±1.2	4.10±0.18	20/24	14±3	8
061324	Mosserud	wave-washed	Sm	50	LA-R	12.6±0.7	50.3±1.7	3.97±0.16	24/24	14±3	16
061325	Mängen	aeolian	Sm	55	LA-R	0.12±0.01	0.52±0.02	4.24±0.18	22/35	21±4	9
061326	Nabbmanen	aeolian	Spc	220	LA-R	10.7±0.6	34.3±0.8	3.22±0.14	24/24	10±2	15
061327	Nabbmanen	aeolian	Spc	180	LA-R	9.2±0.5	34.2±1.2	3.73±0.15	24/24	15±2	14
061328	Nabbmanen	aeolian	Sm	135	LA-R	0.27±0.04	0.99±0.14	3.71±0.27	23/24	44±7	8
061329	Nabbmanen	aeolian	Sm	115	LA-R	0.18±0.01	0.66±0.02	3.65±0.16	24/24	16±3	8
061330	Nabbmanen	aeolian	Sm	65	LA-R	0.18±0.01	0.67±0.02	3.71±0.16	22/22	5±3	9
061331	Nyängen 1	aeolian	Sm	60	LA-R	11.6±0.7	43.0±1.3	3.72±0.16	19/21	10±3	8
061332	Nyängen 1	aeolian	Sm	90	LA-R	10.7±0.7	37.0±1.7	3.47±0.14	22/24	18±3	14
061333	Nyängen 2	wave-washed	Sm	50	LA-R	12.1±0.6	47.1±1.2	3.89±0.16	24/24	9±2	12
061334	Västra höjden	subglacial	D(S)mm	50	LA-R	97.4±6.9	437.9±23.7	4.49±0.19	24/24	25±4	13

^a see Fig. 5 for legend

^b LA-R — large aliquot measured at NLL, Risø; LA-L — large aliquot measured at Lund; SA-L — small (2 mm) aliquot measured at Lund, SA-M — minimum age model (MAM-3) from small aliquots

^c For MAM-3 ages, the value here is the p-value, i.e. the proportion of aliquots that is meaningful

^d Overdispersion

^e measured on the fraction <180 μm (sieve residue from 180–250 μm after chemical preparation) due to lack of material of original fraction

Table 6. Surface exposure sample locations, analytical data and ^{10}Be surface exposure ages.

Sample	Latitude (°N)	Longitude (°E)	Altitude (m a.s.l.)	Thickness (mm)	Topographic and geometric correction factor	^{10}Be exposure age ^a (ka)
ORM-1A	59.6805	13.9421	185	3	1.0000	10.8 ± 0.7 (0.6)
ORM-1B	59.6805	13.9421	185	2	0.9589	11.3 ± 0.8 (0.7)
ORM-2A	59.6805	13.9419	184	1	0.9999	11.7 ± 0.8 (0.7)
ORM-2B	59.6805	13.9419	184	3	0.9527	11.4 ± 1.0 (0.9)
mean						11.3 ± 0.8 (0.7)
ORM-3	59.6805	13.9421	185	2	1.0000	14.4 ± 2.7 (2.6)
VÄS-2	59.67	13.9685	225	2	1.0000	13.2 ± 0.9 (0.7)
VÄS-3	59.6706	13.9681	225	4	0.9643	12.6 ± 0.8 (0.7)
VÄS-4	59.6709	13.9689	224	2	0.9735	12.2 ± 0.7 (0.6)
mean						12.7 ± 0.8 (0.7)

^a Calculated ages are scaled using $e = 0 \text{ mm ka}^{-1}$ and the Lm scheme of the CRONUS online calculator (Balco et al., 2008), wrapper script version 2.2, main calculator version 2.1, constants version 2.2.1, muons version 1.1, with a ^{10}Be half life of 1.387×10^6 years (Chmeleff et al., 2010; Korschinek et al., 2010), and the Arctic calibration data set (Young et al., 2013). A density of 2.7 g cm^{-3} is assumed for all samples. All samples are from the upper surfaces of glacially-deposited boulders. Uncertainties are reported at the 1σ level and include all known sources of analytical and production rate uncertainty. The uncertainties in the parentheses are analytical only.

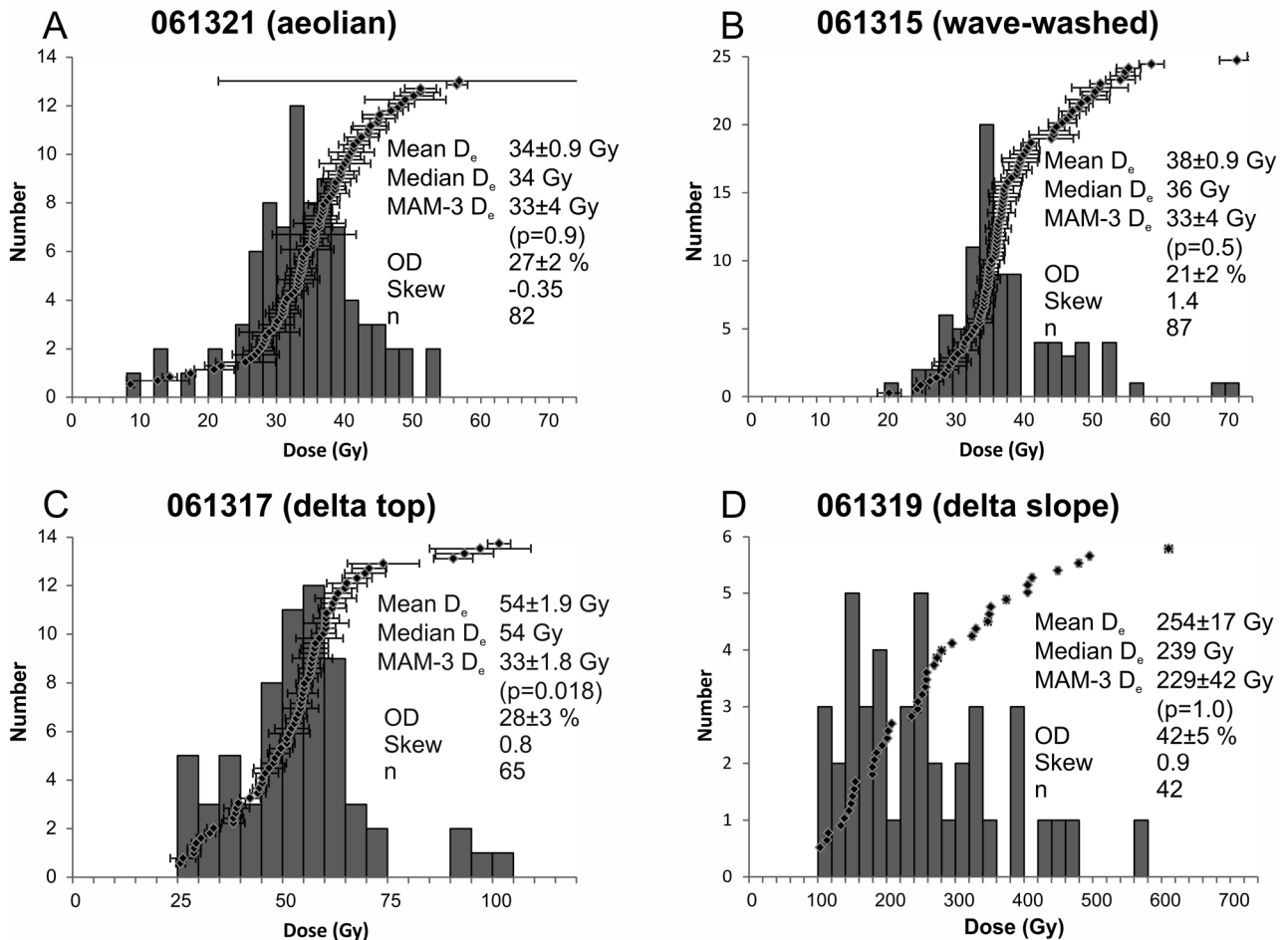


Fig. 7. Small-aliquot dose distributions of samples from different depositional environments. A. Aeolian dune sand from Källorna. B. Wave-washed sand from Hedbacka. C. Delta top sand from Källorna. D. Delta slope sand from Källorna.

Table 7. ^{14}C age from the Nabbmanen site and unpublished ages from Lake Falltjärnen. The ages are calibrated using OxCal 4.2 online and the IntCal13 calibration curve (Bronk Ramsey, 2009; Reimer et al., 2013).

Sample no.	Lab. no.	Material	^{14}C age (^{14}C a BP)	Calibrated age (BP)	Reference
NAB-6	LuS 6814	charcoal	1205±50	1267–989	this study
Falltjärnen	Poz-10380	terrestrial seed	9270±50	10577–10278	Jan Risberg
Falltjärnen	Poz-10381	terrestrial seed	9310±50	10662–10298	Jan Risberg

5. DISCUSSION

Deglaciation

The OSL age of the till at Västra höjden is not expected to give the age of the deglaciation, since till seldom is completely bleached, particularly not subglacial till (Fuchs and Owen, 2008). In this case, the very high equivalent dose (Table 5) supports a subglacial (no bleaching) origin for the till. If it is representative of till in the area, and the till is a likely source material for the glacial deposits, then a comparison of the doses from the till and the deltaic sediments gives some information on the bleaching that has taken place during transport (cf. Alexanderson and Murray, 2012a). The lowermost sample in the delta (at Källorna), which comes from the delta slope, has a dose of ~280 Gy (64% of the till dose), and the uppermost sample, which represents the delta top, has 50 Gy (11%). The decreasing OSL doses and ages upwards in the deltaic succession at Källorna (Fig. 5) may reflect an increased distance to the ice margin and better bleaching opportunities during longer subaerial transport as the delta accreted. This is supported by the two small-aliquot dose distributions from delta sediments; the upper of the two has a lower overdispersion and is slightly less skewed (Fig. 7). The age of the uppermost OSL sample (11.5 ± 0.6 ka) is therefore expected to provide the most reliable age of the deglaciation.

The timing of delta formation, as determined by the OSL age from Källorna, should be contemporaneous with moraine formation and the time when the ice cover disappeared in the area, as represented by the ^{10}Be ages at Ormtjärnen and Västra höjden. This is the case for Källorna (11.5 ± 0.6 ka) and the Ormtjärnen end moraine (11.3 ± 0.8 ka). Both also overlap with the deglaciation age from literature (10.9 cal ka BP; Fredén, 2001a; Lundqvist, 2002). The central mean exposure age for the hummocky moraine at Västra höjden is slightly older (12.7 ± 0.8 ka), but given the uncertainties, the OSL and surface exposure ages are statistically indistinguishable at 1 sigma, even when using only the analytical uncertainties. There are not enough samples to determine if the younger ages are due to post-depositional shielding related to moraine degradation (Heyman et al., 2011; Houmark-Nielsen et al., 2012), or if the older surface exposure ages are caused by nuclide inheritance (e.g. Kelly et al., 2008; Alexanderson et al., 2014). There was no obvious evidence to support either case, but the fact

that the Västra höjden samples are part of a stagnating ice landscape may indicate that the boulders were exposed at the ice surface prior to final deposition, while the samples from the end moraine at Ormtjärnen only started accumulating cosmogenic nuclides once the ice had disappeared. Because of this geological uncertainty we favour the Ormtjärnen surface exposure ages as more closely related to deglaciation.

Land uplift

At Bratthorsheden, the three large-aliquot OSL ages from wave-washed sediments (061315, -24, -33) decrease with altitude from 173 to 145 m a.s.l. (Table 2), as is expected. However, the decrease is at face value only; the three ages are all within error of each other ($12.6\text{--}12.0 \pm 0.7$ ka). They are also at face value older than the deglaciation (11.5–11.3 ka, see above), and therefore overestimate the true age. According to the shoreline displacement curve (Fredén, 2001a), the level of the Yoldia Sea/Ancient Lake Vänern was at these elevations between ~10.6 and ~10 cal ka BP, and so the age overestimation is in the order of 1000–2000 years. The ^{14}C -ages from Lake Falltjärnen are also in line with the ages extracted from the shoreline displacement curve and provide an age of 10.7–10.3 cal ka BP for when the shoreline was at 160–165 m a.s.l. (Table 7).

A likely reason for the age overestimation is incomplete bleaching. Although beach sediments are generally expected to be bleached and to work well for luminescence dating (Jacobs, 2008), experience from Finland shows this is not always the case (Hyttinen et al., 2014). Also, a modern beach close to a glacier in Svalbard had an apparent dose that corresponded to an age overestimate of almost the same order as indicated here, ~400 years (Alexanderson and Murray, 2012b). The overdispersed (21%) and skewed (1.4) small-aliquot dose distribution of sample 061315 (Fig. 7B) supports the incomplete bleaching scenario in this case, and when a statistical age model (MAM-3) is applied to extricate the true age, the age does become younger: 9.5 ± 1.2 ka (Table 5). This younger age — from the lowest site at 145 m a.s.l. — agrees with the ~10 cal ka BP age according to the shoreline displacement curve (Fredén, 2001a).

To avoid incomplete bleaching, careful selection of the facies may help: for example both Argyilan et al. (2005) and Hyttinen et al. (2014) achieved good results from beach-face (foreshore) deposits. However, even if

the beach sediments are bleached and give a consistent OSL chronology (e.g. Nielsen *et al.*, 2006), a limitation of the use of OSL ages to date land uplift is their resolution (Lindén *et al.*, 2006; Fuchs *et al.*, 2012), which generally is less than that of ^{14}C ages. Where organic material is rare, such as in previously glaciated polar areas, and where raised beaches are common, or where luminescence characteristics allow precise ages, OSL dating can be most useful (e.g. Argyilan *et al.*, 2005; Reimann *et al.*, 2010).

Aeolian activity

The oldest aeolian sample age is 11.6 ± 0.7 ka (061331 from Nyängen), but is situated stratigraphically above sample 061332 aged 10.7 ± 0.6 ka. Strictly, the two ages overlap within error and should not be seen as stratigraphically reversed ages. Likely, the age is around 11 ka. This timing is supported by another 10.7 ± 0.6 ka age (lower part of dune at Nabbmanen). From that time on, there is according to our OSL ages ongoing aeolian sedimentation at Brattforsheden until 8.5 ± 0.5 ka (061323). The youngest aeolian age (in this age group) is from cover sand on the southwestern delta plateau (Köldgropen; Fig. 1, Fig. 3). The two TL ages from Finnhöjden and Västerrud 2 (Table 1; Lundqvist and Mejdahl, 1987) agree well with the OSL from the same sites (Table 5).

The minimum age model (MAM) age of the aeolian sample measured with small aliquots (7.8 ± 1.0 ka; 061321) is within error of the mean small-aliquot age, which is expected from a well-bleached sample. However, it can be noted here that the dose distribution of sample 061321 is negatively skewed, i.e. with a low-dose tail, while the MAM is usually applied to positively skewed dose distributions, suspected of incomplete bleaching, to pick out the lowest, best bleached dose population (Galbraith *et al.*, 1999; Bailey and Arnold, 2006). Bateman *et al.* (2003; 2007) have shown at the single-grain level that negatively skewed dose distributions may be due to bioturbation, where young material has been brought to lower stratigraphic levels. Since the MAM identifies the lowest dose population, and would thus incorporate any such too young aliquots in the age calculation, it may give a too young age. Another age model, the central age model (CAM), may therefore be better suited in this case. However, if the CAM is used, the age does not change much, it is 7.9 ± 0.4 ka.

There is no obvious pattern in the spatial distribution of the aeolian deglacial ages within the resolution of the OSL ages. The two sites in the north are $10.7\text{--}9.2 \pm 0.6$ ka and those in the south $10.7\text{--}8.5 \pm 0.7$ ka. Possibly, the aeolian activity, not necessarily dune-forming, may have lasted somewhat longer in the south, but it is only a single site and age. The deposition of the loess-like sediments was also contemporaneous with the formation of the dunes.

It seems therefore that the aeolian deposition started immediately after deglaciation ($11.5\text{--}11.3 \pm 0.8$ ka) and lasted for approximately 2000 years, or somewhat longer. This relatively long duration implies that aeolian activity continued even though vegetation had become established in the area. On a nearby sandplain, Almquist-Jacobson (1994) showed that pioneer vegetation with light-demanding shrubs and herbs dominated until ~ 10.2 cal ka BP, when it was replaced by a semi-open *Pinus* forest until ~ 9.5 cal ka BP. Thereafter forest dominated, although some open areas were present on the sandplain (Almquist-Jacobson, 1994). Nevertheless, as vegetation became more abundant, the sand was eventually stabilised, soils started forming and large-scale aeolian activity ceased.

Interestingly, the survival at Brattforsheden of a post-glacial-maximum relict species, the sand lizard (*Lacerta agilis*), indicates that exposed sand areas have existed continuously in the area since some time during the post-glacial maximum (Gullberg *et al.*, 1998; Berglind, 2005). This in turn suggests that some sand was available for wind transport at Brattforsheden and that aeolian activity may have occurred locally throughout the Holocene. None of this is captured by the current OSL data set, possibly due to the very local scale of the open sand areas.

A palaeosol buried by aeolian sand in the Nabbmanen dune is evidence of re-activation of the aeolian sand. The charcoal in the palaeosol suggests that forest fires, whether natural or human-related, occurred in the area, and these may well have been causing renewed aeolian activity by removing vegetation and exposing sand to the wind. ^{14}C -ages of the charcoal range from 1267–989 to 570–490 cal yr BP (Table 1, Table 7). According to the OSL ages, renewed aeolian activity occurred 270–180 years ago, i.e. starting around AD 1700 and ending about AD 1850. This is a time when it is known from historical records that extensive cutting down of forest took place in the area, related to intensified charcoal production for the smelting industry and to expansion of slash-and-burn agriculture connected to the arrival of Finnish settlers (Furuskog, 1924; von Schoultz, 1984). For example, several crofts are known in the area from around AD 1600 and the Pardixhyttan smeltery, situated just across Lake Alstern from Nabbmanen, was active AD 1629–1873 (Björklund *et al.*, 2003).

The young sand at Nabbmanen has a massive structure and has been interpreted as cover sand draping a dune. It suggests that this young aeolian event rather deposited sand sheets than formed dunes. Hörner (1927) has also observed up to 1.5 m thick ‘lamination free sand’ close to the surface at other dunes and which contained pieces of charcoal; the age of this sand is not known, however.

The youngest aeolian OSL age (061325), apart from the modern analogue, comes from a beach dune at Lake Mången (Fig. 1). This dune is described to have formed

due to lake-level lowering caused by the abandonment of a dam at a local smeltery in the 1700s, and it was stabilised by vegetation in the early 1920s (Furuskog, 1924; Hörner, 1927). The OSL age of 120 ± 10 yr, corresponding to AD 1875–1895, fits well in this time span and confirms the young age of the dune. The low dose and age of a modern analogue — the cliff-top dune formed about 20 years ago at the Källorna gravel pit (50 ± 10 years; 061322) — show that the material can be bleached in nature, supporting the accuracy of the aeolian OSL ages.

6. CONCLUSIONS

Deglaciation in the Brattforsheden area took place $11.3\text{--}11.5 \pm 0.8$ ka ago according to ^{10}Be and OSL dating. This agrees with previous estimates of the time of deglaciation (10.9 cal ka BP). Aeolian dunes started forming directly after deglaciation, and aeolian activity continued for around 2000 years, long after vegetation had become established in the area. During much of the Holocene local open sand patches probably existed within the forested area, but no larger aeolian events were identified or dated within this study. Sand drift started again, at least locally, around 300 years ago and resulted in sand sheets draping the older dunes. This is contemporaneous with intensified human impact on the forest in the area, through charcoal production and slash-and-burn agriculture. OSL ages from glacial, glaciifluvial and wave-washed sediments suffer from incomplete bleaching and overestimate the depositional age. Statistically modelled ages based on small-aliquot dose distributions are only partly able to correct for this. OSL ages from aeolian deposits seem accurate and agree with independent chronological data. The good agreement between OSL ages determined at two different luminescence laboratories (the Nordic Laboratory for Luminescence Dating and the newly established Lund Luminescence Laboratory) also show that OSL measurements are reproducible.

ACKNOWLEDGEMENTS

The field work was carried out when Alexanderson was a research associate at Stockholm University and the laboratory work as a guest researcher at the Nordic Laboratory for Luminescence Dating. The project was funded by the Geological Survey of Sweden (ref. no 60–1356/2005). Several people and organisations have contributed to this project and we wish to acknowledge them: The County Board of Värmland for giving permission to work in the Brattforsheden nature reserve, and particularly Sven-Åke Berglind for the guided tour of the area and the information about the sand lizards. Sven-Allan and Gunnel Alexanderson for their company and help during field work. Tim Johnsen and Jan Risberg, both at Stockholm University, for help with rock crushing and for unpublished ^{14}C ages, respectively. Andrew Murray and

the technical staff at NLL for valued discussions and help with measurements. Martin Bernhardson (Lund University) for providing the hillshade model of Brattforsheden. Henriette Linge (University of Bergen) and Lena Håkansson (Lund University) for discussions on the ^{10}Be ages. The reviewer Frank Preusser for comments that improved the manuscript.

REFERENCES

- Alexanderson H and Murray AS, 2012a. Problems and potential of OSL dating Weichselian and Holocene sediments in Sweden. *Quaternary Science Reviews* 44: 37–50, DOI 10.1016/j.quascirev.2009.09.020
- Alexanderson H and Murray AS, 2012b. Luminescence signals from modern sediments in a glaciated bay, NW Svalbard. *Quaternary Geochronology* 10: 250–256, DOI 10.1016/j.quageo.2012.01.001.
- Alexanderson H, Backman J, Cronin TM, Funder S, Ingólfsson Ó, Jakobsson M, Landvik JY, Löwemark L, Mangerud J, März C, Möller P, O'Regan M and Spielhagen RF, 2014. An Arctic perspective on dating Mid-Late Pleistocene environmental history. *Quaternary Science Reviews* 92: 9–31, DOI 10.1016/j.quascirev.2013.09.023.
- Almquist-Jacobson H, 1994. Interaction of Holocene climate, water balance, vegetation, fire, and cultural land-use in the Swedish Borderland Department of Quaternary Geology, Lund University. PhD thesis LUNDQUA 30. 82 p.
- Aneblom T and Åsman M, 2000. *Beskrivning till kartan över grundvattentillgångarna i Karlstads kommun*, SGU An 8, cd-rom p. Geological Survey of Sweden. [Description to the map of ground water resources in Karlstad municipality]
- Argyilan EP, Forman SL, Johnston JW and Wilcox DA, 2005. Optically stimulated luminescence dating of late Holocene raised strandplain sequences adjacent to Lakes Michigan and Superior, Upper Peninsula, Michigan, USA. *Quaternary Research* 63: 122–135, DOI 10.1016/j.yqres.2004.12.001.
- Arnold LJ, Bailey RM and Tucker GE, 2007. Statistical treatment of fluvial dose distributions from southern Colorado arroyo deposits. *Quaternary Geochronology* 2: 162–167, DOI 10.1016/j.quageo.2006.05.003.
- Bailey RM and Arnold LJ, 2006. Statistical modelling of single grain quartz D_e distributions and an assessment of procedures for estimating burial dose. *Quaternary Science Reviews* 25: 2475–2502, DOI 10.1016/j.quascirev.2005.09.012.
- Balco G, Stone JO, Lifton NA and Dunai TJ, 2008. A complete and easily accessible means of calculating surface exposure ages or erosion rates from ^{10}Be and ^{26}Al measurements. *Quaternary Geochronology* 3: 174–195, DOI 10.1016/j.quageo.2007.12.001.
- Bateman MD, Frederick CD, Jaiswal MK and Singhvi AK, 2003. Investigations into the potential effects of pedoturbation on luminescence dating. *Quaternary Science Reviews* 22: 1169–1176, DOI 10.1016/S0277-3791(03)00019-2.
- Bateman MD, Boulter CH, Carr AS, Frederick CD, Peter D and Wilder M, 2007. Detecting post-depositional sediment disturbance in sandy deposits using optical luminescence. *Quaternary Geochronology* 2: 57–64, DOI 10.1016/j.quageo.2006.05.004.
- Berglind S-Å, 2005. *Population dynamics and conservation of the sand lizard (Lacerta agilis) on the edge of its range*. Department of Evolution, Genomics and Systematics, Uppsala University. PhD thesis Acta Universitatis Upsaliensis, Digital Comprehensive Summaries of Uppsala Dissertations from the Faculty of Science and Technology 41. 42 p.
- Bergqvist E, 1981. *Svenska inlandsdyner, Översikt och förslag till dynreservat*Rapport, 103 p. Statens naturvårdsverk. In Swedish. [Ancient inland dunes in Sweden Survey and proposals for dune reserves]
- Bergqvist E and Lindström E, 1971. Bevis på subrecent eolisk aktivitet på Brattforshedens inlandsdyner (Evidence for subrecent aeolian activity on the Brattforsheden inland dunes). *Geologiska*

- Föreningens i Stockholm Förhandlingar 93: 782–785, DOI 10.1080/11035897109451550. In Swedish.
- Bevington PR and Robinson DK, 1992. *Data reduction and error analysis for the physical sciences*. McGraw-Hill, New York.
- Björklund P, Langhof J and Berg L, 2003. *Värmlandsberg. Atlas över svensk bergslag* (Värmlandsberg. Atlas of Swedish mining districts). Jernkontoret, Stockholm. In Swedish.
- Bronk Ramsey C, 2009. Bayesian analysis of radiocarbon dates. *Radiocarbon* 51: 337–360.
- Child D, Elliott G, Mifsud C, Smith AM and Fink D, 2000. Sample processing for earth science studies at ANTARES. *Nuclear Instruments and Methods in Physics Research Section B, Beam Interactions with Materials and Atoms* 172: 856–860, DOI 10.1016/S0168-583X(00)00198-1.
- Chmeleff J, von Blanckenburg F, Kossert K and Jakob D, 2010. Determination of the ^{10}Be half-life by multicollector ICP-MS and liquid scintillation counting. *Nuclear Instruments and Methods in Physics Research Section B: Beam Interactions with Materials and Atoms* 268: 192–199, DOI 10.1016/j.nimb.2009.09.012.
- Duller GAT, 2003. Distinguishing quartz and feldspar in single grain luminescence measurements. *Radiation Measurements* 37: 161–165, DOI 10.1016/S1350-4487(02)00170-1.
- Fenton CR, Hermanns RL, Blikra LH, Kubik PW, Bryant C, Niedermann S, Meixner A and Goethals MM, 2011. Regional ^{10}Be production rate calibration for the past 12 ka deduced from the radiocarbon-dated Grøtlandsura and Russenes rock avalanches at 69° N, Norway. *Quaternary Geochronology* 6: 437–452, DOI 10.1016/j.quageo.2011.04.005.
- Fredén C, 2001a. *Beskrivning till jordartskartan 11D Munkfors SO (Description to the Quaternary map 11D Munkfors SE)*, SGU Ae 150, 76 p. Geological Survey of Sweden, Uppsala. In Swedish with English summary.
- Fredén C, 2001b. *Jordartskartan 11D Munkfors SO (Quaternary map 11D Munkfors SE)*. Geological Survey of Sweden. SGU Ae 150.
- Fuchs M and Owen LA, 2008. Luminescence dating of glacial and associated sediments: review, recommendations and future directions. *Boreas* 37: 636–659, DOI 10.1111/j.1502-3885.2008.00052.x.
- Fuchs M, Kreutzer S, Fischer M, Sauer D and Sørensen R, 2012. OSL and IRSL dating of raised beach sand deposits along the southeastern coast of Norway. *Quaternary Geochronology* 10: 195–200, DOI 10.1016/j.quageo.2011.11.009.
- Furuskog J, 1924. *De värmländska järnbruksbygderna (The Värmland ironworks districts)*. Bronnellska bokhandeln, Filipstad. PhD thesis Lund University. In Swedish.
- Galbraith RF, Roberts RG, Laslett GM, Yoshida H and Olley JM, 1999. Optical dating of single and multiple grains of quartz from Jinmium rock shelter, northern Australia. Part I: experimental design and statistical models. *Archaeometry* 41: 339–364, DOI 10.1111/j.1475-4754.1999.tb00987.x.
- Goehring BM, Lohne ØS, Mangerud J, Svendsen JI, Gyllencreutz R, Schaefer J and Finkel R, 2012a. Erratum: Late glacial and holocene ^{10}Be production rates for western Norway. *Journal of Quaternary Science* 27: 544–544, DOI 10.1002/jqs.2548.
- Goehring BM, Lohne ØS, Mangerud J, Svendsen JI, Gyllencreutz R, Schaefer J and Finkel R, 2012b. Late glacial and holocene ^{10}Be production rates for western Norway. *Journal of Quaternary Science* 27: 89–96, DOI 10.1002/jqs.1517.
- Gullberg A, Olsson M and Tegelström H, 1998. Colonization, genetic diversity, and evolution in the Swedish sand lizard, *Lacerta agilis* (Reptilia, Squamata). *Biological Journal of the Linnean Society* 65: 257–277, DOI 10.1111/j.1095-8312.1998.tb01142.x.
- Heyman J, Stroeven AP, Harbor JM and Caffee MW, 2011. Too young or too old: Evaluating cosmogenic exposure dating based on an analysis of compiled boulder exposure ages. *Earth and Planetary Science Letters* 302, 71–80, DOI 10.1016/j.epsl.2010.11.040.
- Houmark-Nielsen M, Linge H, Fabel D, Schnabel C, Xu S, Wilcken KM and Binnie S, 2012. Cosmogenic surface exposure dating the last deglaciation in Denmark: Discrepancies with independent age constraints suggest delayed periglacial landform stabilisation. *Quaternary Geochronology* 13: 1–17, DOI 10.1016/j.quageo.2012.08.006.
- Hyttinen O, Eskola KO, Kaakinen A and Salonen V-P, 2014. First direct age determination for the Baltic Ice Lake/Yoldia Sea transition in Finland. *GFF* 136: 398–405, DOI 10.1080/11035897.2013.813581.
- Högbom I, 1923. Ancient Inland Dunes of Northern and Middle Europe. *Geografiska Annaler* 5: 113–243.
- Hörner NG, 1927. Brattförsheden ett värmländskt randdeltekomplex och dess dyner (Brattförsheden a complex of wash plains or marginal deltas and its dunes). Geological Survey of Sweden. SGU C342. 206 p. In Swedish with English summary.
- Jacobs Z, 2008. Luminescence chronologies for coastal and marine sediments. *Boreas* 37: 508–535, DOI 10.1111/j.1502-3885.2008.00054.x.
- Kelly MA, Lowell TV, Hall BL, Schaefer JM, Finkel RC, Goehring BM, Alley RB and Denton GH, 2008. A ^{10}Be chronology of lateglacial and Holocene mountain glaciation in the Scoresby Sund region, east Greenland: implications for seasonality during lateglacial time. *Quaternary Science Reviews* 27: 2273–2282, DOI 10.1016/j.quascirev.2008.08.004.
- Klemsdal T, 1969. Eolian Forms in Parts of Norway. *Norsk Geografisk Tidsskrift* 23: 49–66.
- Kohl CP and Nishiizumi K, 1992. Chemical isolation of quartz for measurement of *in-situ*-produced cosmogenic nuclides. *Geochimica et Cosmochimica Acta* 56: 3583–3587, DOI 10.1016/0016-7037(92)90401-4.
- Korschinek G, Bergmaier A, Faestermann T, Gerstmann UC, Knie K, Rugel G, Wallner A, Dillmann I, Dollinger G, von Gostomski CL, Kossert K, Maiti M, Poutivtsev M and Remmert A, 2010. A new value for the half-life of ^{10}Be by Heavy-Ion Elastic Recoil Detection and liquid scintillation counting. *Nuclear Instruments and Methods in Physics Research Section B: Beam Interactions with Materials and Atoms* 268: 187–191, DOI 10.1016/j.nimb.2009.09.020.
- Lindén M, Möller P, Björck S and Sandgren P, 2006. Holocene shore displacement and deglaciation chronology in Norrbotten, Sweden. *Boreas* 35: 1–22, DOI 10.1111/j.1502-3885.2006.tb01109.x.
- Lundqvist J, 1958. *Beskrivning till jordartskarta över Värmlands län (Description to the Quaternary deposits map of Värmland county)*, SGU Ca 38, 229 p. Geological Survey of Sweden. In Swedish.
- Lundqvist J, 2002. Weichseltidens huvudfas. In: Fredén C (Ed.) *Berg och jord (The main phase of the Weichselian)*, Sveriges Nationalatlas. pp. 124–135. (in Swedish).
- Lundqvist J and Mejdahl V, 1987. Thermoluminescence dating of eolian sediments in central Sweden. *Geologiska Föreningens i Stockholm förhandlingar* 109: 147–158, DOI 10.1080/11035898709453764.
- Lundqvist J and Wohlfarth B, 2001. Timing and east-west correlation of south Swedish ice marginal lines during the Late Weichselian. *Quaternary Science Reviews* 20: 1127–1148, DOI 10.1016/S0277-3791(00)00142-6.
- Magnusson NH and Assarsson G, 1929. *Beskrivning till kartbladet Nyed (Description to the map sheet Nyed)*, SGU Aa 144, 108 p. Geological Survey of Sweden, Stockholm. In Swedish.
- Murray AS and Wintle AG, 2000. Luminescence dating of quartz using an improved single-aliquot regenerative-dose protocol. *Radiation Measurements* 32: 57–73, DOI 10.1016/S1350-4487(99)00253-X.
- Murray AS and Wintle AG, 2003. The single aliquot regenerative dose protocol: potential for improvements in reliability. *Radiation Measurements* 37: 377–381, DOI 10.1016/S1350-4487(03)00053-2.
- Murray AS, Marten R, Johnson A and Martin P, 1987. Analysis for naturally occurring radionuclides at environmental concentrations by gamma spectrometry. *Journal of Radioanalytical and Nuclear Chemistry Articles* 115: 263–288, DOI 10.1007/BF02037443.
- Nielsen A, Murray AS, Pejrup M and Elberling B, 2006. Optically stimulated luminescence dating of a Holocene beach ridge plain in Northern Jutland, Denmark. *Quaternary Geochronology* 1: 305–312, DOI 10.1016/j.quageo.2006.03.001.

- Nishiizumi K, Imamura M, Caffee MW, Southon JR, Finkel RC and McAninch J, 2007. Absolute calibration of ^{10}Be AMS standards. *Nuclear Instruments and Methods in Physics Research Section B: Beam Interactions with Materials and Atoms* 258: 403–413, DOI 10.1016/j.nimb.2007.01.297.
- Plug LJ, Gosse JC, McIntosh JJ and Bigley R, 2007. Attenuation of cosmic ray flux in temperate forest. *Journal of Geophysical Research: Earth Surface* 112: F02022, DOI 10.1029/2006jf000668.
- Prescott JR and Hutton JT, 1994. Cosmic ray contributions to dose rates for luminescence and ESR dating: large depths and long-term time variations. *Radiation Measurements* 23: 497–500, DOI 10.1016/0277-3791(95)00037-2.
- Reimann T, Naumann M, Tsukamoto S and Frechen M, 2010. Luminescence dating of coastal sediments from the Baltic Sea coastal barrier-spit Darss-Zingst, NE Germany. *Geomorphology* 122: 264–273, DOI 10.1016/j.geomorph.2010.03.001.
- Reimer PJ, Bard E, Bayliss A, Beck JW, Blackwell PG, Bronk Ramsey C, Buck CE, Cheng H, Edwards RL, Friedrich M, Grootes PM, Guilderson TP, Haflidason H, Hajdas I, Hatté C, Heaton TJ, Hoffmann DL, Hogg AG, Hughen KA, Kaiser KF, Kromer B, Manning SW, Niu M, Reimer RW, Richards DA, Scott EM, Southon JR, Staff RA, Turney CSM and van der Plicht J, 2013. IntCal13 and Marine13 Radiocarbon Age Calibration Curves 0–50,000 Years cal BP. *Radiocarbon* 55: 1869–1887, DOI 10.2458/azu_js_rc.55.16947.
- Seppälä M, 1972. Location, Morphology and Orientation of Inland Dunes in Northern Sweden. *Geografiska Annaler. Series A, Physical Geography* 54: 85–104.
- Singarayer JS, Bailey RM, Ward S and Stokes S, 2005. Assessing the completeness of optical resetting of quartz OSL in the natural environment. *Radiation Measurements* 40: 13–25, DOI 10.1016/j.radmeas.2005.02.005.
- SMHI, 2014. Normalt största snödjup under vintern, medelvärde 1961-1990 (Normal largest snow depth during winter, mean value 1961-1990). Swedish Meteorological and Hydrological Institute. <http://www.smhi.se/klimatdata/meteorologi/sno/Normalt-storsta-snodjup-under-vintern-medelvarde-1.7931>, accessed 2014-04-05. In Swedish.
- von Schoultz G, 1984. *Värmländsk historia (The history of Värmland)*. Norstedts, Stockholm. In Swedish.
- Young NE, Schaefer JM, Briner JP and Goehring BM, 2013. A ^{10}Be production-rate calibration for the Arctic. *Journal of Quaternary Science* 28: 515–526, DOI 10.1002/jqs.2642.